International Scientific Conference 20 UNITECH 26

INTERNATIONAL SCIENTIFIC CONFERENCE
19-21 November 2026
GABROVO

EFFECT OF COOLING RATE ON SOLIDIFICATION AND MICROSTRUCTURAL PROPERTIES OF SILVER NANOPARTICLES

Unal Domekeli[1], Murat Celtek[2], Cem Canan[3]

[1]Dept. of Physics, Trakya University, 22030, Edirne – Türkiye
[2]Faculty of Education, Trakya University, 22030, Edirne – Türkiye
[3]Edirne Vocational College of Technical Science, Trakya University, 22030, Edirne – Türkiye
……
**Corresponding author: unaldomekeli@trakya.edu.tr*

Abstract
Metallic nanoparticles have become a significant research topic in both fundamental scientific research and advanced technology applications due to their size-dependent and unique properties. Besides their broad application potential in mechanical, magnetic, electronic, and biomedical fields, the nanoscale solidification process determines the final microstructure and properties of the material. Therefore, understanding the solidification mechanism at the atomic scale is crucial, especially for additive manufacturing processes based on rapid solidification. In this study, the atomic and microstructural changes occurring in silver (Ag) nanoparticles under rapid cooling conditions were investigated using molecular dynamics (MD) simulations. Simulations used an initial liquid nanoparticle consisting of a total of 10192 Ag atoms, and the solidification behavior of the system was monitored at different cooling rates. The characteristic changes in the system's potential energy during cooling were used to determine the solidification temperatures. Furthermore, the resulting atomic structure after solidification was investigated through pair distribution functions (PDF), Honeycutt–Andersen (HA) pair analyses, and direct visualization of atomic configurations. The results showed that the cooling rate is crucial for the solidification behavior and final atomic structure of Ag nanoparticles. Crystalline structure formation was observed at low cooling rates (0.1–1.0 K/ps), while glassy structure formation was promoted at high cooling rates (≥10.0 K/ps) by limiting atomic rearrangement. These findings reveal that cooling rate is one of the fundamental parameters determining the final microstructure of nanoscale Ag systems.

Keywords: Ag nanoparticle, MD simulations, solidification, cooling rate.

INTRODUCTION

Nanometer-sized metallic structures exhibit different thermal and physical behaviors than bulk materials due to their high surface-to-volume ratio [1]. One of the most striking features of these structures is the significant decrease in their melting temperatures compared to their bulk counterparts [2]. In addition, their mechanical, electrical, magnetic and optical properties make them important materials for advanced technology applications [3–5]. Therefore, metallic nanoparticles (NPs) are used in the development of functional materials for bonding and joining processes, especially in electronic packaging technologies. Mold bonding and inkjet printing-based applications can be given as examples of these application areas [6]. Since rapid temperature changes during additive manufacturing determine the atomic configurations and thermal behavior of metallic NPs, understanding the heat transfer mechanisms at the nano-scale is of great importance. However, experimental methods have limitations in directly and thoroughly investigating the atomic movements and structural transformations that occur in these processes. Atomistic simulations are used as a complement to experimental studies by enabling the modeling of physical events at different

This is an open access article licensed under Creative Commons Attribution 4.0 International
Print ISSN: 1313-230X, Online ISSN: 3033-1404

scales to overcome these limitations [7]. In this context, the MD simulation technique contributes to the explanation of the physical mechanisms underlying additive manufacturing by tracking the interactions between atoms and their evolution over time [6]. Many studies [6,8–11] have shown that cooling rate is one of the main parameters determining the structural properties of metallic nanoparticles during the cooling process and after solidification. For example, Vo et al. [6] investigated the solidification temperature and atomic structure of Ag nanoparticles using MD simulations for different cooling rates and particle sizes. They showed that increasing the cooling rate reduced the ratio of face-centered cubic (fcc) and hexagonal closed packed (hcp) structures and that glassy structures formed above a certain critical rate. They also reported that the ratio of tightly packed structures increased with increasing particle size. Based on these findings, in this study, the effects of changes in cooling rate on the structural evolution and solidification and glass transition processes of Ag NPs with 10192 atoms (7.0 nm in diameter) were systematically analyzed through MD simulations conducted based on EAM potential.

EXPOSITION

In the atomic-level study of metallic systems, accurate characterization of interatomic interactions is crucial. For this purpose, EAM considers not only binary atomic interactions but also the multiple-body contributions of surrounding atoms when calculating system energy. This feature allows EAM potentials to be widely used in MD simulations that investigate the atomic behavior of metallic systems. Within the scope of the EAM approach, the total energy of a system consisting of N atoms is defined by the following equation [12,13]:

$$E_{tot} = \sum_{i=1}^{N}\left[\frac{1}{2}\sum_{i\neq j}^{N}\phi(r_{ij}) + F_i(\rho_i)\right], \qquad (1)$$

where the $\phi(r_{ij})$ term describes the pairwise interaction between atoms i and j, while the $F_i(\rho_i)$ term represents the embedding energy required to place atom i at a position with an electron density of ρ_i. ρ_i denotes the total electron density generated by neighboring atoms surrounding atom i, and r_{ij} represents the distance between atoms i and j. In modeling the interactions between Ag–Ag atoms, the EAM potential dataset proposed by Sheng [14] was used. In this study, the atomic-scale behavior of Ag NPs was investigated using the DL_POLY parallel simulation-package [15]. A spherical NP model with a diameter of 7.0 nm and containing 10192 atoms was used in the simulations. The initial structure was created by cutting a spherical particle from a fcc crystal lattice. The solid NP was heated from 100 K to 1800 K at a rate of 0.1 K/ps and equilibrated at this temperature for 100 ps to allow the formation of the liquid phase. To investigate the effect of cooling rate on structural transformations, the nanoparticle was cooled from 1800 K to 100 K using three different cooling rates: 0.1, 1, and 10 K/ps. Periodic boundary conditions were not applied in the simulations to preserve the free surface effects of the nanoparticle. All nanoparticle simulations were performed in the NVT ensemble representing constant particle number, volume, and temperature conditions. The equations of motion of the atoms were solved using the Leapfrog–Verlet algorithm with a time step of 1 fs; the system temperature was controlled via a Nose–Hoover thermostat [16].

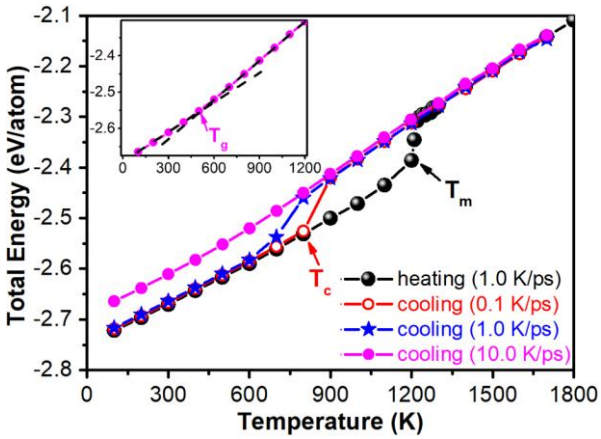


Fig. 1. *Temperature dependence of the total energy of Ag NPs.*

The transition temperature of an NP from liquid to solid phase can be determined by examining the temperature-dependent variation of thermodynamic parameters. Figure 1 presents the total energy profiles obtained from MD simulations performed at different cooling rates for liquid Ag NP, along with the heating process curve. During the heating process, the total energy of the system increases proportionally with the temperature increase until it reaches the melting temperature (T_m). The first-order phase transformation that occurs at this temperature is manifested as a significant jump in the energy profile. After melting, the total energy of the liquid phase continues its linear increase with temperature. During the cooling process, the structural transformation of the system can be determined from the character of the energy curve. In the cooling processes, the total energy decreases with decreasing temperature. The sharp energy drops in the curves obtained at rates of 0.1 and 1 K/ps are related to the transformation of the liquid phase into a crystalline solid. The temperatures at which these transformations occur are expressed as the solidification temperature (T_c). However, increasing the cooling rate to 10 K/ps eliminates the sudden drop in the energy profile and causes a significant divergence in the slope of the curve. This suggests that rapid cooling prevents crystallization, leading to the solidification of NP in a glassy structure. Under these conditions, the glass transition temperature (T_g) is calculated from the intersection of the congruence lines applied to the linear sections of the energy curve at different temperature ranges (see inset of Figure 1). T_m, T_c and T_g temperatures determined from the simulations are given in Table 1. The results show that increasing the cooling rate lowers the temperature at which solidification occurs.

Table 1. *T_g, T_c and T_m temperatures of Ag NP.*

Rate	T_g (K)	T_c (K)	T_m (K)
10 K/ps (cooling)	520	---	---
1.0 K/ps (cooling)	---	700	---
0.1 K/ps (cooling)	---	800	---
1.0 K/ps (heating)	---	---	1210

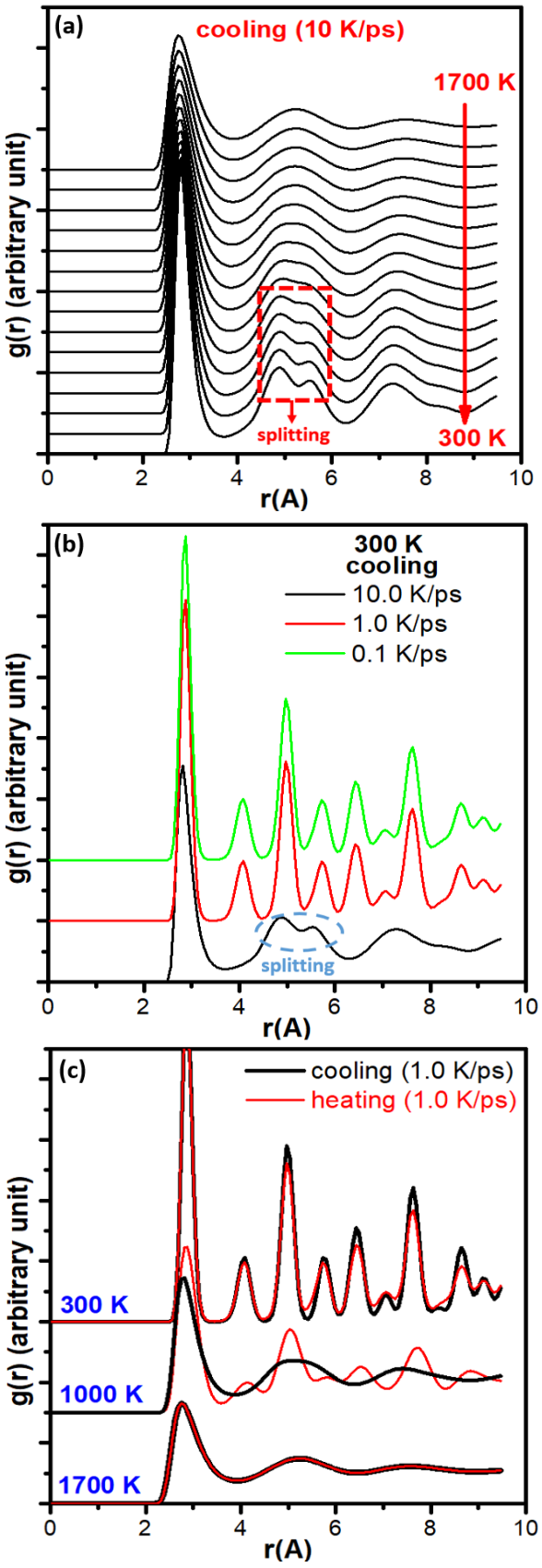


Fig. 2. *(a) PDFs of Ag NPs cooled at a cooling rate of 10 K/ps, (b) PDFs of Ag NPs obtained at different cooling rates at 300 K, (c) PDFs calculated for Ag NPs at different temperatures with heating and cooling rates of 1 K/ps.*

To reveal the structural transformations that Ag NP undergoes during rapid cooling, the atomic arrangement obtained at different temperatures can be analyzed using multiple methods. In this context, atomic configurations obtained from MD simulations, PDF and HA analysis can be used together to evaluate the atomic structure and phase changes in the system. PDF, $g(r)$, which is used to determine whether the material has crystalline, liquid or glassy character, can be obtained through the following expression [17]:

$$g(r) = \frac{V}{N^2}\langle(\sum_{i=1}^{N} n_i(r))/4\pi r^2 \Delta r\rangle, \qquad (2)$$

where, V and N parameters represent the unit cell volume and the total number of atoms in the simulation system, respectively. Figure 2(a) shows the PDF curves of Ag NPs obtained at different temperatures with a cooling rate of 10 K/ps. In the temperature range of 1700–800 K, the curves exhibit structural features specific to the liquid phase. The splitting that appears in the second peak at 800 K becomes more pronounced around the T_g temperature. The splitting observed in the second peak of the PDF curve obtained at 300 K after the cooling process is one of the characteristic features of amorphous structures. This finding supports the transformation of the liquid Ag NPs into a glassy structure with a cooling rate of 10 K/ps. Figure 2(b) presents a comparative PDF profile of Ag NPs obtained at a temperature of 300 K with cooling rates of 0.1, 1, and 10 K/ps. The PDF curves of NPs cooled at rates of 0.1 and 1 K/ps exhibit characteristics consistent with fcc crystal structure. As the cooling rate increases, the heights of the PDF peaks decreases while the peak widths increase. In contrast, the PDF curve of the NPs cooled at 10 K/ps differs from the profiles obtained under the other two conditions due to the cleavage that becomes apparent in the second peak. The atomic structural changes of the Ag NP during heating and cooling processes were investigated through PDF profiles calculated at a rate of 1 K/ps and temperatures of 300, 1000, and 1700 K, as shown in Figure 2(c). The overlap between the results obtained for 300 K and 1700 K in both thermal processes reveals that the atomic order at these temperatures is similar. However, a significant difference is observed between the two processes at 1000 K. The fact that the PDF exhibits solid-phase characteristics during heating and maintains its liquid-phase character during cooling reflects the different structural states of the system in the hysteresis region. This indicates that phase transitions depend not only on temperature but also on the thermal process followed by the system. The PDF profiles obtained after cooling suggest the formation of an atomic structure similar to the fcc crystal order in the Ag NP. However, since PDF analysis does not directly reveal the three-dimensional properties of atomic coordination, this similarity is not sufficient for a definitive characterization of the crystal structure. Therefore, in order to evaluate the local atomic arrangement and crystal structure properties of the nanoparticle in more detail, the PDF findings need to be considered together with HA analysis.

HA pair analysis is used to determine the local geometric arrangement and microstructural features in atomic systems [8,18]. In this approach, the neighborhood relationships around pairs of atoms are defined by an index system expressed with four digits. In this representation (i,j,k,l), the first component indicates whether there is a bond between the atoms under investigation; the presence of a bond is indicated by 1, and its absence by 2. The second component represents the number of common neighbors shared by the two atoms, and the third component represents the number of bonds between these neighbors. The fourth component is used to distinguish local atomic arrangements that have the same first three components. Thanks to this indexing system, different atomic configurations can be associated with specific HA bond types. In the system under investigation, the index 1551 is used to define the ideal icosahedral (icos) arrangement, while the indices 1541

and 1431 are used to define defective icosahedral (deficos) configurations. In distinguishing crystalline phases, the 1421 index is associated with the fcc structure, while the combined evaluation of 1421 and 1422 bond types allows for the determination of the hcp order. The characteristic indicators of the bcc crystal structure are the 1661 and 1441 indices. Atom pairs outside the structures defined by these indices are classified under other bond types that cannot be included in a specific structural class.

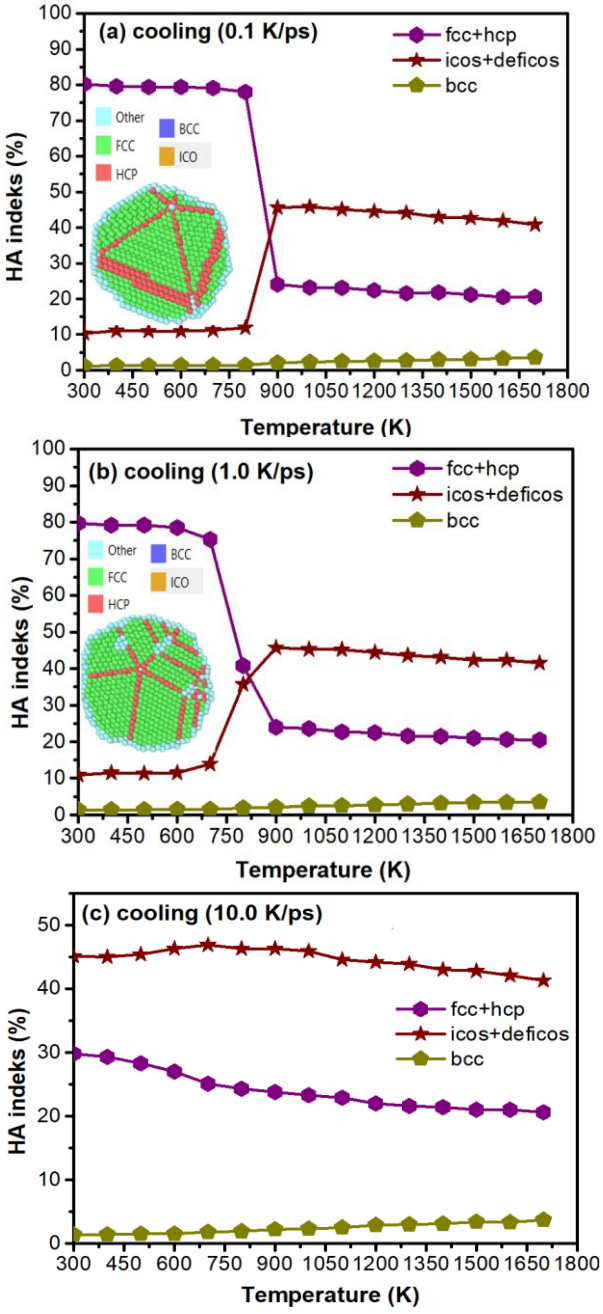


Fig. 3. *Temperature-dependent variation of the HA index of Ag NP at various cooling rates.*

The effect of different cooling conditions on the structural transformation of Ag NPs was investigated through the temperature-dependent variation of HA indices obtained from MD simulations. Figures 3(a) and (b) show the results obtained for cooling rates of 0.1 K/ps and 1 K/ps. In both cases, a sharp change in the distribution of atomic structures is observed around the temperature T_c. Below this temperature, the total proportion of fcc and hcp structures associated with crystal order increases significantly, while the proportion of atomic environments classified as icos and deficos decreases. In contrast, there is no significant change in the proportion of atoms belonging to the bcc structure during solidification. When the cooling process reaches 300 K, it is observed that in both conditions, the total proportion of fcc and hcp structures is higher than that of other local structure types. Common Neighbor Analysis (CNA) was used to spatially examine the local coordination properties of atoms and to visually support the structural changes determined by HA analysis. The inset images in Figure 3(a) and (b) show the cross-sections of the nanoparticles formed after solidification and the classified distribution of atoms according to their local crystal structures. CNA results confirm the coexistence of regions with fcc and hcp orderings within the nanoparticle. In addition, the locations and distributions of planar defects between different crystal regions can also be determined through this analysis. Therefore, the final structure obtained at 300 K does not consist of only a single type of crystal ordering; it exhibits a complex microstructure in which the fcc structure is dominant, including hcp regions and other atomic configurations corresponding to short-range ordering. This structural diversity reveals the polycrystalline character of the solidified Ag NP. Figure 3(c) shows that icos and deficos species are dominant at a cooling rate of 10 K/ps, and their proportions increase as the temperature decreases. Below T_g temperature, the fcc+hcp ratio increases

while the bcc ratio remains largely constant. The high proportion of icos and deficos species at 300 K indicates that the NP has transformed into a glassy structure and supports the PDF analysis results.

CONCLUSION

This study investigated the microstructural changes of 7.0 nm diameter Ag NP containing 10192 atoms during cooling and the effect of cooling rate on solidification temperature using MD simulations. The results show that in the range of 0.1–10 K/ps, the NPs transform predominantly into a polycrystalline structure with an fcc structure, while at the critical cooling rate of 10 K/ps, a tendency towards glassy structure formation emerges. Furthermore, it was determined that the solidification temperature decreases with increasing cooling rate. These findings reveal that cooling rate is an important parameter affecting the solidification process and final microstructure of Ag NPs.

ACKNOWLEDGMENTS: *We would like to thank Trakya University Rectorate for giving permission and contributing to present this study as a paper.*

REFERENCE

[1] F.G. Shi, Size dependent thermal vibrations and melting in nanocrystals, J. Mater. Res. 9 (1994) 1307–1314.
[2] K.K. Nanda, Size-dependent melting of nanoparticles: Hundred years of thermodynamic model, Pramana 72 (2009) 617–628.
[3] N. Wang, Z. Wang, K.T. Aust, U. Erb, Effect of grain size on mechanical properties of nanocrystalline materials, Acta Metall. Mater. 43 (1995) 519–528.
[4] C. Stephenson, A. Hubler, Stability and conductivity of self assembled wires in a transverse electric field, Sci. Rep. 5 (2015) 15044.
[5] L. LaConte, N. Nitin, G. Bao, Magnetic nanoparticle probes, Mater. Today 8 (2005) 32–38.
[6] T.Q. Vo, B. Kim, A molecular dynamics study on cooling rate effect on atomic structure of solidified silver nanoparticles, Eur. Phys. J. D 73 (2019) 183.
[7] R. Van Noorden, Modellers react to chemistry award, Nature 502 (2013) 280–280.
[8] Cem Canan, Murat Celtek, Unal Domekeli, Molecular dynamics simulation study on the structural evolution of liquid nickel nanoparticles during rapid cooling, UNITECH-2025 – Sel. Pap. (2025).
[9] A. Mahata, M.A. Zaeem, M.I. Baskes, Understanding homogeneous nucleation in solidification of aluminum by molecular dynamics simulations, Model. Simul. Mater. Sci. Eng. 26 (2018) 025007.
[10] T. D. Nguyen, C.C. Nguyen, V.H. Tran, Molecular dynamics study of microscopic structures, phase transitions and dynamic crystallization in Ni nanoparticles, RSC Adv. 7 (2017) 25406–25413.
[11] S. Yasushi, A Molecular Dynamics Study of Effects of Size and Cooling Rate on the Structure of Molybdenum Nanoparticles, J. Therm. Sci. Technol. 7 (2012) 45–57.
[12] M.S. Daw, M.I. Baskes, Embedded-atom method: Derivation and application to impurities, surfaces, and other defects in metals, Phys. Rev. B 29 (1984) 6443–6453.
[13] Unal Domekeli, Arda Kolcular, A molecular dynamics simulation study of the melting behaviour of iridium nanoparticles, UNITECH-2025 – Sel. Pap. (2025).
[14] H. Sheng, EAM potentials, (2026). https://sites.google.com/site/eampotentials/ag.
[15] W. Smith, T.R. Forester, DL_POLY_2.0: A general-purpose parallel molecular dynamics simulation package, J. Mol. Graph. 14 (1996) 136–141.
[16] S. Nose, A unified formulation of the constant temperature molecular dynamics methods, J. Chem. Phys. 81 (1984) 511–519.
[17] U. Domekeli, M. Celtek, A Molecular Dynamics Simulation Study of the Melting and Solidification Processes of Hafnium Nanoparticles, Langmuir 42 (2026) 28003–28016.
[18] J. D. Honeycutt, H.C. Andersen, Molecular dynamics study of melting and freezing of small Lennard-Jones clusters, J. Phys. Chem. 91 (1987) 4950–4963.